Int J Clin Exp Med 2016;9(2):736-744
www.ijcem.com /ISSN:1940-5901/IJCEM0018800

Original Article

Dynamic volume computed tomography perfusion imaging in evaluation of secondary ischemia after acute cerebral hemorrhage

Rui Li, Yuxia Duan, Kuikui Zheng, Qiuyun Tong, Zilong Hu, Jinjin Liu, Guoquan Cao, Yunjun Yang, Qichuan Zhuge, Jing Xue, Weijian Chen

Department of Radiology / Molecular and Digital Medical Imaging Institute, The First Affiliated Hospital of Wenzhou Medical University; Zhejiang Provincial Key Laboratory of Aging and Neurological Disorder Research, Wenzhou 325000, China

Received October 29, 2015; Accepted January 15, 2016; Epub February 15, 2016; Published February 29, 2016

Abstract: This study aims to investigate the use of 320-slice volume computed tomography perfusion imaging (VCTPI) for evaluation of secondary cerebral ischemia after acute supratentorial spontaneous cerebral hematoma. VCTPI data of 33 patients with acute supratentorial spontaneous cerebral hematoma were retrospectively analyzed. Perfusion parameters in affected tissues, surrounding tissues, and corresponding contralateral mirror image zones were analyzed, and ipsilateral/contralateral relative values were calculated for each parameter. The paired t test was used to compare the differences among the parameters. The perfusion in the affected regions was reduced in comparison to the mirror image regions, and differences in cerebral blood flow (CBF), cerebral blood volume (CBV), mean transit time (MTT), and time-to-peak (TTP) were all statistically significant. CBF and TTP in ipsilateral non-affected areas were significantly lower than that in the contralateral mirror image regions, but the differences in CBV and MTT between sides were not significant. There were visible perfusion asymmetries between the cerebellar hemispheres in 10 of 33 patients (30%), 8 of whom exhibited reduced perfusion in the hematoma-contralateral cerebellum and 2 of whom exhibited reduced perfusion in the hematoma-ipsilateral cerebellum. The tissues surrounding acute supratentorial spontaneous cerebral hematoma were hypoperfused. VCTPI not only displayed secondary cerebral ischemia around the hematoma, but also revealed changes distant to the primary lesion, thus achieving a comprehensive assessment of post-hemorrhagic cerebral perfusion.

Keywords: Brain diseases, tomography, X-ray computer, perfusion

Introduction

Spontaneous cerebral hemorrhage is a common neurological emergency that accounts for 10% to 15% of all stroke events [1-5]. It has greater mortality and morbidity than other stroke subtypes [1, 6]. Clinical studies have shown that cerebral hemorrhage results in mechanical damage caused by the space occupying effects of the hematoma itself as well secondary injury around the hematoma, both of which are instrumental to the mortality and morbidity of brain hemorrhage [7, 8]. Previous studies have shown that computed tomography perfusion imaging (CTPI) has an important diagnostic role in cases of cerebral hematoma, especially towards describing hemodynamic changes in the surrounding tissues [1, 3-6]. However, previous CTPI technologies could not image the entire brain, thus lesions distal to the site of the hemorrhage might not be shown completely or could be missed entirely. More recently, whole-brain perfusion imaging has gradually replaced traditional CTPI [9, 10]. Technologies such as 320-slice dynamic volume CTPI (VCTPI) can achieve whole-brain perfusion imaging in one scan, thus allowing comprehensive assessment of the cerebral hematoma itself as well as both surrounding tissues and distant parts. In this study, the value of whole brain perfusion imaging by 320-slice VCTPI in diagnosing secondary cerebral ischemia after cerebral hematoma was assessed in 33 patients with acute supratentorial spontaneous cerebral hematoma.

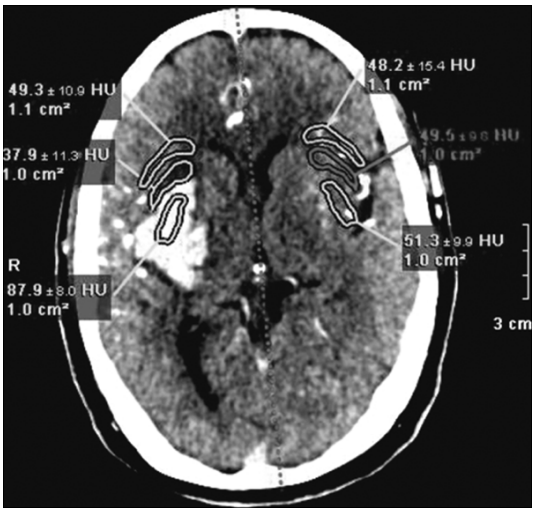

Figure 1. Male, 59 years old, suddenly occurred the left limb weakness for 10 h, the plain CT scanning revealed the hematoma in right basal ganglion. ROI was drawn manually, measured the CBF, CBV, MTT and TTP values of PA and NA; then set the cerebral midline as the mirror, and drew ROI in the healthy side of contralateral hemisphere, and the corresponding perfusion parameters were measured.

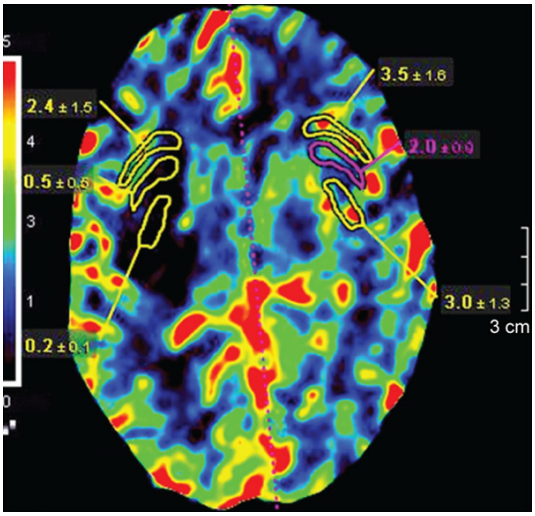

Figure 2. Right-left PA: CBV 0.5 ml·(100 g)$^{-1}$·min^{-1} vs 2.0 ml·(100 g)$^{-1}$·min^{-1}, right-left NA: CBV 2.4 ml·(100 g)$^{-1}$·min^{-1} vs 3.5 ml·(100 g)$^{-1}$·min^{-1}; CBV was increasingly decreased in right PA and NA.

Materials and methods

Patients

Patients who were diagnosed with acute spontaneous cerebral hemorrhage and underwent VCTPI at the First Affiliated Hospital of Wenzhou Medical University from July 2013 to January 2015 were enrolled in this retrospective analysis. The inclusion criteria were: (1) supratentorial acute (within 72 h) spontaneous cerebral hemorrhage; (2) accompanied with sudden limb weakness with (or without) headache and vomiting associated with (or without) slurred speech; (3) images acquired within the acute period using the Toshiba Aquilion ONE 320-slice Dynamic Volume CT scanner (Toshiba, Yokohama, Japan); (4) absence of iodine allergy and heart, liver, and kidney dysfunction; and (5) signed informed consent. Exclusion criteria were: (1) hemorrhage caused by intracranial aneurysm, vascular malformation, cerebral infarction, brain tumor, and brain trauma; (2) CT angiography-confirmed presence of significant cerebral arterial stenosis (including the cerebellar artery); (3) organic cerebral parenchymal lesions; (4) iodine allergy, heart, liver, or kidney dysfunction; and (5) excessive motion or restlessness during the examination process that might affect image quality. A total of 33 patients, 21 men and 12 women aged 22 to 79 years (average 55.79 years), met the inclusion criteria, among whom 20 patients had a history of hypertension, 16 had basal ganglionic hemorrhage, and 17 had lobar hemorrhage. This study was conducted in accordance with the declaration of Helsinki. This study was conducted with approval from the Ethics Committee of Wenzhou Medical University. Written informed consent was obtained from all participants.

Computed tomography protocol

The Aquilion ONE 320-slice CT scanner was used, and all patients underwent one-stop cranial CT examination. The single-lap rotation time of head CTPI was 0.75 s. The scanning tube voltage was 100 kV with a tube current of 150 to 310 mA. A 50 mL bolus of Omnipaque 350 mgI/mL non-ionic contrast agent (GE Pharmaceutical Co., Ltd. Shanghai, China) was injected via the antecubital vein at a rate of 4 to 5 mL/s, followed by 20 mL of saline at the same rate. The scanning interval was 2 s for the arterial phase and 5 s for the venous phase and the total scan time was approximately 60 s. During the scanning process, the head was fixed with head fixation band. Each scan produced a total of 19 sets of volume data with 320 images in each set, for a total of 6080 images. Image thickness was 0.5 mm.

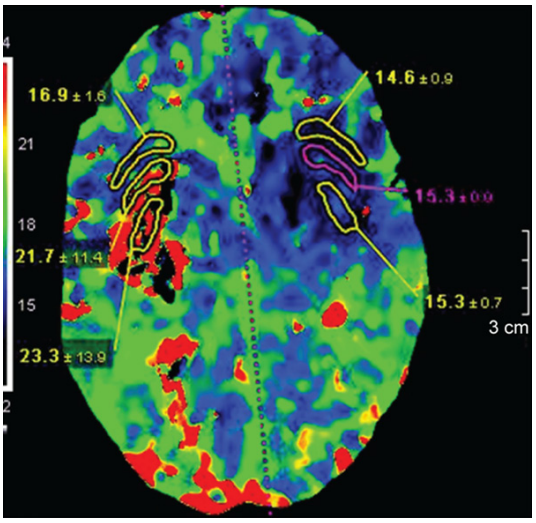

Figure 3. Right-left PA: TTP 21.7 s vs. 15.3 s, right-left NA: TTP 16.9 s vs. 14.6 s; TTP was extended in right PA.

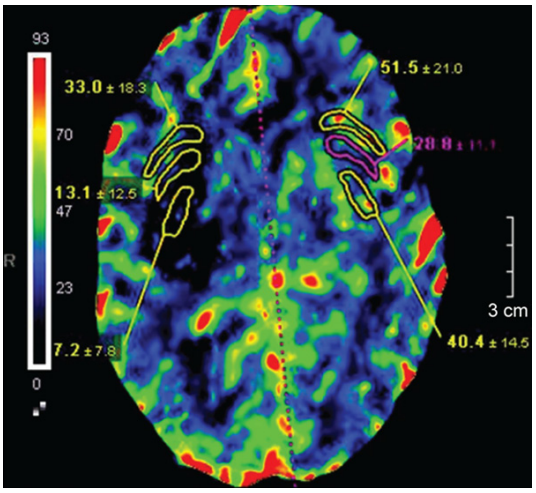

Figure 4. Right-left PA: CBF13.1 ml·(100 g)$^{-1}$·min^{-1} vs 28.8 ml·(100 g)$^{-1}$·min^{-1}, right-left NA: CBF33.0 ml·(100 g)$^{-1}$·min^{-1} vs. 51.5 ml·(100 g)$^{-1}$·min^{-1}; CBF was increasingly decreased in right PA and NA.

Calculation of radiation dose

The dose-length product (DLP) of the head was displayed on the machine during the one-stop CT examination was recorded and multiplied with the effective dose coefficient ([0.0023][3]) to obtain the total effective radiation dose for each patient.

Image post-processing and data acquisition

All the data were input into a Toshiba 4D-DSA software package for automatic subtraction,

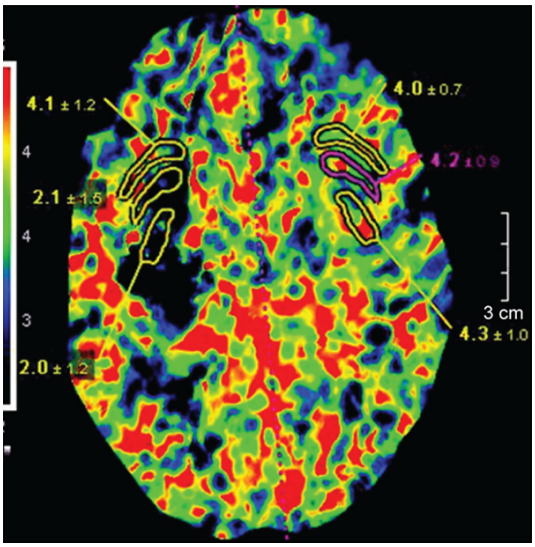

Figure 5. Right-left PA: MTT 2.1 s vsv4.2 s, right-left NA: MTT 4.1 s vs. 4.0 s, MTT was shortened in right PA.

followed by regeneration of 3D dynamic vascular images, application of pseudo-color, arbitrary-angle rotation, and local enlargement or shielding that allowed blood vessels to be much more clearly displayed. The software measured the volume of the hematoma and all of the data were then imported into the Vetrea 3 software skull analysis module, which automatically generated whole brain enhanced three-dimensional (3D) color images from which regional cerebral blood flow (CBF), regional cerebral blood volume (CBV), mean transit time (MTT), and time-to-peak (TTP) could be determined. Enhancements were based on each patient's actual situation and the region of interest (ROI) of (100±10) mm^2 was set manually (**Figures 1-5**). CBF, CBV, MTT, and TTP were measured in the perihematomal low-density area (PA) and in the normal-appearing brain tissue (NA) within 1 cm surrounding the PA. The same perfusion parameters were checked in a mirror ROI that was drawn at the same distance from the cerebral midline in the contralateral hemisphere and relative (rCBF, rCBV, rMTT, and rTTP) values of the tissue perfusion parameters were calculated from the ratio (ipsilateral/contralateral) of perfusion parameters in each ROI (**Figures 2-5**). All measurements were repeated three times and results for the absolute value and relative value of each parameter are expressed as mean ± standard deviation.

Table 1. Comparison of perfusion parameters of PA and MPA in the 33 patients ($\bar{x}$±s)

Observation region	CBF [ml•(100 g)$^{-1}$•min^{-1}]	CBV (ml/100 g)	MTT (s)	TTP (s)
PA	16.83±5.89	1.04±0.41	3.70±0.93	20.16±3.07
MPA	24.18±6.67	1.71±0.35	4.44±0.75	17.74±3.78
t	-11.223	-11.743	-4.641	5.035
P	0.000	0.000	0.000	0.000

Table 2. Comparison of perfusion parameters of NA and MNA in the 33 patients ($\bar{x}$±s)

Observation region	CBF [ml•(100 g)$^{-1}$•min^{-1}]	CBV (ml/100 g)	MTT (s)	TTP (s)
NA	24.53±6.97	1.77±0.38	4.51±0.74	17.98±3.49
MNA	26.09±7.40	1.85±0.41	4.47±0.8	17.63±3.58
t	-3.586	-2.007	0.662	2.62
P	0.001	0.053	0.512	0.013

Table 3. Comparison of relative values of perfusion parameters of PA and NA in the 33 patients ($\bar{x}$±s)

Perfusion parameter	rCBF	rCBV	rMTT	rTTP
PA	0.70±0.14	0.61±0.20	0.84±0.17	1.16±0.19
NA	0.95±0.10	0.98±0.15	1.02±0.09	1.02±0.05
t	-8.747	-9.057	-5.639	4.399
P	0.000	0.000	0.000	0.000

Statistical analysis

SPSS17.0 statistical software was used for the data processing. The measurement data met the normal distribution, and therefore the paired t test was to compare the differences of different parameters in their corresponding cerebral regions during the acute phase, and the paired-sample t test was performed to compare the differences of relative values of various perfusion parameters in their corresponding cerebral regions. $P<0.05$ indicated statistical significance.

Results

Perfusion parameters in the perihematomal low density area

Among the 33 patients, the largest volume of cerebral hematoma was 94.45 mL, while the minimal volume was 5.72 mL, and the average volume was 31.75 mL. The acute phase values of CBF, CBV, MTT, and TTP in the perihematomal low density area (PA) were 16.83±5.89 mL·100 g^{-1}·min^{-1}, 1.04±0.41 mL/100 g, 3.70±0.93 s, and 20.16±3.07 s, and the values in the corresponding mirror area (MPA) were 24.18±6.67 mL·100 g^{-1}·min^{-1}, 1.71±0.35 mL/100 g, 4.44±0.75 s, and 17.74 ±3.78 s, respectively. The perfusion to the PA was significantly reduced, with comparison values of perfusion parameters (PA-MPA) as follows: tCBF = -11.223, $P_{CBF}<0.01$; tCBV = -11.743, $P_{CBV}<0.01$; tMTT = -4.641, $P_{MTT}<0.01$, and tTTP = 5.035, $P_{TTP}<0.01$ (**Table 1**).

Perfusion parameters in normal-appearing brain

In the acute phase, the CBF, CBV, MTT, and TTP values of normal appearing brain in the 1 cm surrounding the PA (NA) were 24.53 ±6.97 mL·100 g^{-1}·min^{-1}, 1.77±0.38 mL/100 g, 4.51 ±0.74 s, and 17.98±3.49 s, and the values in the corresponding mirror area (MNA) were 26.09±7.40 mL·100 g^{-1}·min^{-1}, 1.85±0.41 mL/100 g, 4.47±0.80 s, and 17.63±3.58 s, respectively. The differences in CBF and TTP between NA and MNA (NA-MNA) were significantly different (tCBF = -3.586, $P_{CBF}<0.01$ and tTTP = 2.620, $P_{TTP}<0.05$), but the differences in CBV and MTT values were not (tCBV = -2.007, $P_{CBV}>0.05$ and tMTT = 0.662, $P_{MTT}>0.05$) (**Table 2**).

Relative values of perfusion parameters

In the acute phase, the rCBF, rCBV, rMTT, and rTTP values for the perihematomal low density area (PA) were 0.70±0.14, 0.61 ±0.20, 0.84±0.17, and 1.16±0.19, The corresponding values for the normal appearing tissue in the surrounding 1 cm (NA) were 0.95±0.10, 0.98±0.15, 1.02±0.09, and 1.02±0.05. The differences in rCBF and rCVP between PA and NA (PA-NA) were significant (trCBF = -8.747, $P_{rCBF}<0.01$ and trCBV = -9.057, $P_{rCBV}<0.01$), and rMTT in the PA was relatively shorter than rMTT

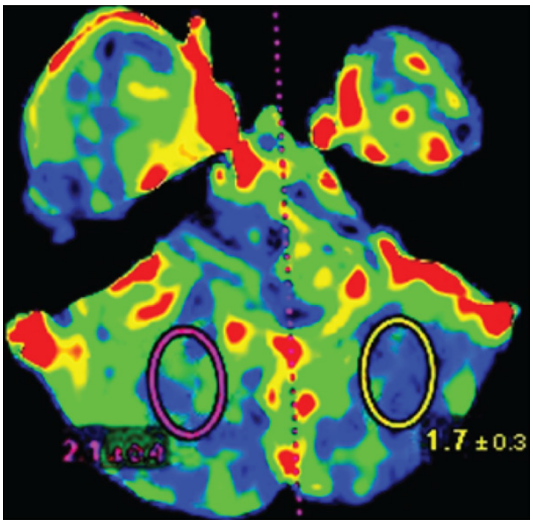

Figure 6. CBV on cerebellar level, right-left CBV: 2.1 ml·(100 g)$^{-1}$·min^{-1} vs. 1.7 ml·(100 g)$^{-1}$·min^{-1}; CBV was reduced in the left.

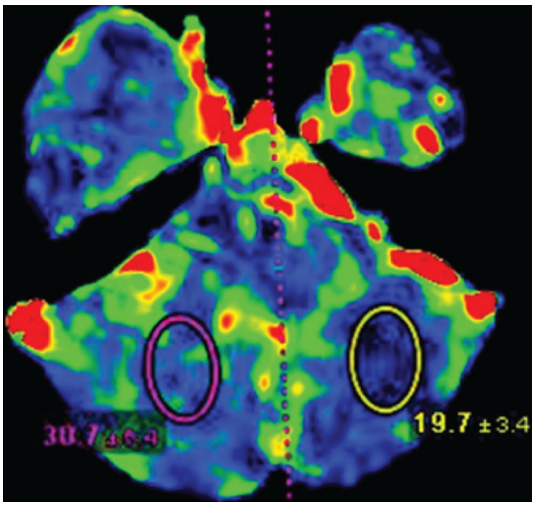

Figure 8. CBF on cerebellar level, right-left CBF: 30.7 ml·(100 g)$^{-1}$·min^{-1} vs. 19.7 ml·(100 g)$^{-1}$·min^{-1}, CBF was decreased in the left.

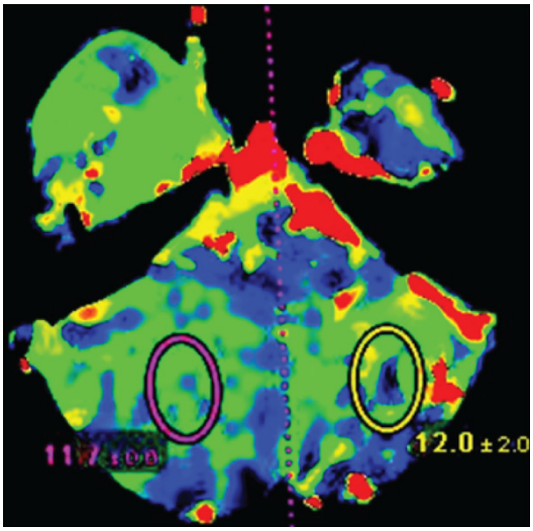

Figure 7. TTP on cerebellar level, right-left TTP: 11.7 s vs. 12.0 s, TTP was slightly longer in the left.

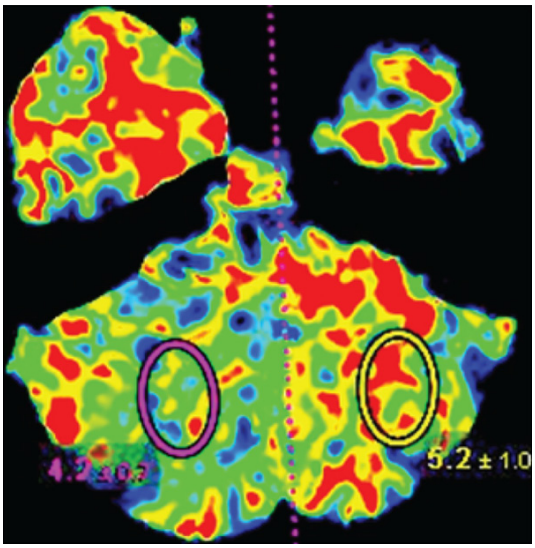

Figure 9. MTT on cerebellum level, right-left MTT: 4.2 s vs. 5.2 s, MTT was extended in the left.

in the NA (trMTT = -5.639, P_{rMTT}<0.01) while rTTP was longer (trTTP = 4.399, P_{rTTP}<0.01) (**Table 3**).

Perfusion abnormalities in cerebellar hemispheres

There were 10 patients (10/33; 30%) who had visible perfusion asymmetry between the cerebellar hemispheres on VCTPI (**Figures 6**-**9**). Of these, 8 patients (24%, 8/33) exhibited reduced perfusion in the cerebellar hemisphere opposite the hematoma. The CBF values of the hematoma-contralateral cerebellum ranged from 20.0 to 45.3 mL·100 g^{-1}·min^{-1}, CBV from 1.5 to 2.8 mL/100 g, MTT from 3.1 to 7.8 s, and TTP from 13.7 to 21.7 s. CBF values in hematoma-ipsilateral cerebellum ranged from 22.2 to 45.7 mL·100 g^{-1}·min^{-1}, CBV from 1.6 to 3.0 mL/100 g, MTT from 3.0 to 7.3 s, and TTP from 13.3 to 21.1 s. There were 2 patients (6%, 2/33) who exhibited reduced perfusion in the hematoma-ipsilateral cerebellar hemispheres, with CBF values in the hematoma-ipsilateral cerebellum ranging from 21.6 to 33.6 mL·100

g^{-1}·min^{-1}, CBV from 2.2 to 3.0 mL/100 g, MTT from 5.3 to 6.1 s, and TTP from 10.6 to 17.3 s, and CBF values in the hematoma-contralateral cerebellum ranging from 21.8 to 35.0 mL·100 g^{-1}·min^{-1}, CBV from 2.1 to 3.5 mL/100 g, MTT from 5.0 to 6.5 s, and TTP from 9.8 to 16.2 s.

Radiation dose

The DLP of the one-stop cranial CT examination was 4244.30 mGy with an effective radiation dose as about 9.76 mSv.

Discussion

Cerebral hemorrhage is a devastating type of stroke. The high mortality and morbidity are closely related to the mechanical damage caused by the space-occupying effects of the hematoma itself as well as to secondary injury to surrounding tissues [5, 11, 12]. The pathological mechanisms of secondary cerebral ischemia are complex. A number of studies [3-6, 8, 13-15] have shown that the tissues around the cerebral hematoma exhibit different degrees of hypoperfusion, which is closely related to prognosis. It was generally thought that in the early stage of cerebral hemorrhage, the hypoperfusion of the surrounding tissues was related to the space-occupying effects of the hematoma itself, and that with the development of the hematoma, retraction of blood clots and generation of hematoma cleavage products, toxicities of blood components, and associated inflammation might be leading factors in subsequent brain injury [15, 16]. Zazulia et al. [17] used positron emission tomography (PET) to examine 19 patients with small hematomas, and found that in 16 patients with no midline shift, the CBF and the cerebral metabolic rate of oxygen ($CMRO_2$) in the periclot area were significantly lower than CBF and $CMRO_2$ in the contralateral mirror region in the acute stage of intracerebral hemorrhage. The reduction in $CMRO_2$ was greater than the reduction of CBF, suggesting that factors other than the mass effect from the hematoma were responsible for the surrounding ischemic changes. Herweh et al. [18] have also interpreted the reduced perfusion as a secondary phenomenon, i.e., as result of reduced oxygen demand of tissue damaged by pressure and clot components and not as the cause of any tissue damage associated with acute intracerebral hemorrhage. We believed that it was not sufficient to explain perihematomal hypoperfusion after cerebral hemorrhage as a function of reduced oxygen metabolism, and Herweh thought that the reduced perfusion and reperfusion during the acute stage of cerebral hemorrhage might cause the neuronal damage that could in turn aggravate the tissue ischemia. Beseoglu et al. [11] agreed that the perihematomal tissues were at risk of secondary cerebral damage after cerebral hemorrhage, and found that the volume of lobar hematoma was associated with regions of perihematomal perfusion. Beseoglu proposed that perihematomal hypoperfusion was most likely to be caused by increased local tissue pressures, which thus resulted in autoregulation failure and metabolic imbalance in small arteries and capillary smooth muscle. Removing the hematoma reduced the local tissue pressures and improved the perfusion [16].

CTPI provides multiple hemodynamic parameters that can quantitatively reflect hypoperfusion status, and because it can overcome the shortcomings of other imaging techniques, it has become an ideal method to study the dynamics of perihematomal blood flow. CBF and CBV are two very important hemodynamic parameters of CTPI, and can accurately reflect the perfusion state of perihematomal tissues. In the present study, which included 33 patients with supratentorial cerebral hemorrhage, the areas around the hematoma, particularly the perihematomal low density area (PA), had lower CBV, CBF, and MTT values than the contralateral mirror areas (**Figures 2**, **4**, **5**), while TTP was prolonged (**Figure 3**). These results confirmed the existence of low perfusion around the cerebral hematoma and are consistent with the results of previous studies [3] which also found that perihematomal hypoperfusion exhibited a gradient-like change and that perfusion values were gradually improved from the bleeding core to the periphery areas, as indicated by negative correlation with the distance to the hematoma. In the present study relative perfusion (rCBF and rCBV) was lower in the PA that in the normal-appearing tissues in the surrounding 1 cm (**Figures 2**, **4**), which also suggests a gradual improvement of perfusion with increasing distance from the center to the perihematomal area.

It is generally accepted that MTT reflects the rate of flow of the contrast agent through the

capillaries, thus providing good predictability towards perfusion abnormalities in the brain that could sensitively exhibit the reduction of local perfusion pressures at the distal vascular end. Normally, the ischemic band might exhibit a prolonged MTT, but the results of the present study concerning the above point of view were inconsistent with a previous study [3]. Visual assessment of perfusion and the measured values all showed that the rMTT of the PA in comparison to its contralateral mirror (MPA) was extended, rather than shortened (**Figure 5**). This may be because different technologies were used in the two studies, thus, different perfusion algorithms resulted in the different results. Previous studies have often used a deconvolution algorithm to obtain the values of hemodynamic parameters, while in the present the Toshiba Aquilion ONE 320-slice 640-layer CT scanner added the concept of delay-insensitive singular value decomposition (SVD +) based on the original layer. MTT represents the amount of time that blood stays inside the capillary and is based on the amount of time between the arterial enhanced peak and the tissue enhanced peak, which is then subdued by the delay while the delay represents the relative time of arrival of the contrast agent at the tissue voxel, which is different than the original definition of MTT. However, whether this is the reason for the MTT and rMTT findings in the present study that is contrary to previous studies will need to be confirmed in the future. TTP is a the more sensitive parameter, and in the present study, the TTP parametric figure and all of the measured values clearly showed that TTP was prolonged in the PA, and the rTTP of the PA was also prolonged compared to that of NA (**Figure 3**), and this finding is similar to that reported previously.

Clinically, in order to prevent the continuous expansion of the hematoma and to improve the prognosis in the acute stage of cerebral hemorrhage, rapid treatment to lower the blood pressure has been a common measure, but because of the perihematomal ischemic changes, many authors have recently expressed concern that rapid reduction in blood could aggravate the problem of ischemia during the acute phase, and have also reported that lowering the blood pressure in the early stage did not significantly affect the cerebral blood flow of the perihematomal area [6, 19-21].

The one-stop cranial CT examination can obtain a plain CT scan along with whole-brain CTPI and CTA images. The total radiation dose from the Aquilion ONE 320-slice scanner used in the present study was 9.76 mSv, and when controlling the image quality, the tube current, tube voltage, and scanning time could be appropriately adjusted to further reduce the radiation dose. Previously reported radiation doses [22-24] for whole-brain CTP examination were 5.1 mSv, 6.7 to 7.5 mSv, and 11.2 mSv, and in studies of traditional brain perfusion imaging that included CT scan + CTP + CTA (one-stop examination) radiation doses varied according to the scanning parameters, scanning time, layer numbers, and other settings. Because of restrictions imposed by the detector thickness of some CT scanners, the CTPI examination only included two levels, namely the basal ganglion and the caudomedial part of the lateral ventricle [15]. In these conditions, with a scan time of 40 s, the total effective dose range reached 5.96 to 7.81 mSv. When examiners selected 4 layers with the basal ganglion as the center and covered 2 upper layers and 2 lower layers, with a layer thickness of about 2 cm, the radiation dose was 10 to 15 mSv or higher.

Because the total thickness covered by older CTPI technologies was only about 2 to 4 cm, evaluations of cerebral hematomas usually included only the layers with larger hematomal cross-sectional area, which might have resulted in missed lesions or signs of injury outside the CTP scanning range. The 320-slice CTPI encompasses the whole brain with a coverage range of up to 16 cm, and it is equipped with whole-brain 4D perfusion intelligent clinical analysis software that can automatically generate the color pictures and perfusion data of arbitrary coronal, sagittal, and axial sections of the whole brain, from the cerebellum to the parietal lobe, including CBF, CBV, MTT, and TTP, thus providing major advances toward assessing the functional status of the entire brain after intracerebral hemorrhage. In the present study cerebellar perfusion asymmetries were detected in 10 patients (30%, 10/33). The reduced cerebellar perfusion was on the side opposite the hematoma in 8 of these patients (24%, 8/33) (**Figures 6**-**9**) and on the same side in 2 patients (6%, 2/33), and it might have been a harbinger of cerebellar diaschisis. This change has rarely been detected previously

[25, 26], possibly because traditional CTP could not cover the cerebellum, therefore contributing to the misdiagnosis of this phenomenon. Therefore, whole-brain VCTPI not only reveals hypoperfusion around the perihematomal brain tissues, but is also useful for evaluation of the perfusion status of distant brain tissues, which could undoubtedly facilitate the implementation of individualized treatment programs, and would also have profound clinical impacts.

Acknowledgements

National "12th five-year" Technology Support Program (2011BAI08B09); Wenzhou Municipal Science and Technology Project (Y20140029).

Disclosure of conflict of interest

None.

Address correspondence to: Weijian Chen, Department of Radiology / Molecular and Digital Medical Imaging Institute, The First Affiliated Hospital of Wenzhou Medical University; Zhejiang Provincial Key Laboratory of Aging and Neurological Disorder Research, No. 2 Fuxue Road, Wenzhou 325000, China. Tel: +86 577 88069577; Fax: +86 577 55559661; E-mail: weijianchencn@126.com

References

[1] Sun SJ, Gao PY, Sui BB, Hou XY, Lin Y, Xue J and Zhai RY. "Dynamic spot sign" on CT perfusion source images predicts haematoma expansion in acute intracerebral haemorrhage. Eur Radiol 2013; 23: 1846-1854.

[2] Kashefiolasl S, Foerch C and Pfeilschifter W. Graphite furnace atomic absorption spectrophotometry--a novel method to quantify blood volume in experimental models of intracerebral hemorrhage. J Neurosci Methods 2013; 213: 147-150.

[3] Fainardi E, Borrelli M, Saletti A, Schivalocchi R, Azzini C, Cavallo M, Ceruti S, Tamarozzi R and Chieregato A. CT perfusion mapping of hemodynamic disturbances associated to acute spontaneous intracerebral hemorrhage. Neuroradiology 2008; 50: 729-740.

[4] Long CX and Guo Q. CT perfusion imaging on cerebral hemorrhage haematoma around low perfusion is reviewed. Int J Neurol Neurosurg 2010; 37: 384-387.

[5] Hou XY and Gao PY. Perihematomal perfusion typing and spot sign of acute intracerebral hemorrhage with multimodecomputed tomography: a preliminary study. Chin Med Sci J 2014; 29: 139-143.

[6] El Ahmadieh TY, El Tecle NE, Lall RR, Park AE and Bendok BR. Blood pressure control for spontaneous intracerebral hemorrhage: does blood pressure control causeperihematoma ischemia? Neurosurgery 2013; 72: N14-N16.

[7] Fülesdi B, Réka Kovács K, Bereczki D, Bágyi P, Fekete I and Csiba L. Computed tomography and transcranial Doppler findings in acute and subacute phases of intracerebralhemorrhagic stroke. J Neuroimaging 2014; 24: 124-130.

[8] Orakcioglu B, Kentar MM, Schiebel P, Uozumi Y, Unterberg A and Sakowitz OW. Perihemorrhagic ischemia occurs in a volume-dependent manner as assessed by multimodal cerebral monitoring in a porcine model of intracerebral hemorrhage. Neurocrit Care 2015; 22: 133-139.

[9] Murayama K, Katada K, Nakane M, Toyama H, Anno H, Hayakawa M, Ruiz DS and Murphy KJ. Whole-brain perfusion CT performed with a prototype 256-detector row CT system: initial experience. Radiology 2009; 250: 202-211.

[10] Page M, Nandurkar D, Crossett MP, Stuckey SL, Lau KP, Kenning N and Troupis JM. Comparison of 4 cm Z-axis and 16 cm Z-axis multidetector CT perfusion. Eur Radiol 2010; 20: 1508-1514.

[11] Beseoglu K, Etminan N, Turowski B, Steiger HJ and Hänggi D. The extent of the perihemorrhagic perfusion zone correlates with hematoma volume in patients with lobar intracerebral hemorrhage. Neuroradiology 2014; 56: 535-541.

[12] Mayer SA, Lignelli A, Fink ME, Kessler DB, Thomas CE, Swarup R and Van Heertum RL. Perilesional blood flow and edema formation in acute intracerebral hemorrhage: a SPECT study. Stroke 1998; 29: 1791-1798.

[13] Rosand J, Eskey C, Chang Y, Gonzalez RG, Greenberg SM and Koroshetz WJ. Dynamic single-section CT demonstrates reduced cerebral blood flow in acute intracerebral hemorrhage. Cerebrovasc Dis 2002; 14: 214-220.

[14] Yang GY, Betz AL, Chenevert TL, Brunberg JA and Hoff JT. Experimental intracerebral hemorrhage: a relationship between brain edema, blood flow, and blood-brain barrier permeability in rats. J Neurosurg 1994; 81: 93-102.

[15] Xu HZ, Chen WJ, Wang MH, Cao GQ, Duan YX and Zhu JY. CT Perfusion imaging predicts one-month outcome in patients with acute spontaneous hypertensive intracerebral hemorrhage. Advances in Computed Tomography 2013; 2: 107-111.

[16] Etminan N, Beseoglu K, Turowski B, Steiger HJ and Hänggi D. Perfusion CT in patients with spontaneous lobar intracerebral hemorrhage: effect of surgery on perihemorrhagic perfusion. Stroke 2012; 43: 759-763.

[17] Zazulia AR, Diringer MN, Videen TO, Adams RE, Yundt K, Aiyagari V, Grubb RL Jr and Powers WJ. Hypoperfusion without ischemia surrounding acute intracerebral hemorrhage. J Cereb Blood Flow Metab 2001; 21: 804-810.

[18] Herweh C, Jüttler E, Schellinger PD, Klotz E, Jenetzky E, Orakcioglu B, Sartor K and Schramm P. Evidence against a perihemorrhagic penumbra provided by perfusion computed tomography. Stroke 2007; 38: 2941-2947.

[19] Gould B, McCourt R, Gioia LC, Kate M, Hill MD, Asdaghi N, Dowlatshahi D, Jeerakathil T, Coutts SB, Demchuk AM, Emery D, Shuaib A and Butcher K; ICH ADAPT Investigators. Acute blood pressure reduction in patients with intracerebral hemorrhage does not result in border-zone region hypoperfusion. Stroke 2014; 45: 2894-2899.

[20] Olivot JM, Mlynash M, Kleinman JT, Straka M, Venkatasubramanian C, Bammer R, Moseley ME, Albers GW and Wijman CA; DASH investigators. MRI profile of the perihematomal region in acute intracerebral hemorrhage. Stroke 2010; 41: 2681-2683.

[21] Butcher KS, Jeerakathil T, Hill M, Demchuk AM, Dowlatshahi D, Coutts SB, Gould B, McCourt R, Asdaghi N, Findlay JM, Emery D and Shuaib A; ICH ADAPT Investigators. The intracerebral hemorrhage acutely decreasing arterial pressure trial. Stroke 2013; 44: 620-626.

[22] Brouwer PA, Bosman T, van Walderveen MA, Krings T, Leroux AA and Willems PW. Dynamic 320-section CT angiography in cranial arteriovenous shunting lesions. AJNR Am J Neuroradiol 2010; 31: 767-770.

[23] Siebert E, Bohner G, Masuhr F, Deuschle K, Diekmann S, Wiener E, Bauknecht HC and Klingebiel R. Neuroimaging by 320-row CT: is there a diagnostic benefit or is it just another scanner? A retrospective evaluation of 60 consecutive acute neurological patients. Neurol Sci 2010; 31: 585-593.

[24] San Millan Ruiz D, Murphy K and Gailloud P. 320-multidetector row whole-head dynamic subtracted CT angiography and whole-brain CT perfusion before and after carotid artery stenting: technical note. Eur J Radiol 2010; 74: 413-419.

[25] Orrison WW Jr, Snyder KV, Hopkins LN, Roach CJ, Ringdahl EN, Nazir R and Hanson EH. Whole-brain dynamic CT angiography and perfusion imaging. Clin Radiol 2011; 66: 566-574.

[26] Wu YT, Chang ST, Chen LC and Li TY. Concurrence of crossed cerebellar diaschisis and parakinesia brachialis oscitans in a patient with hemorrhagic stroke. Case Rep Med 2013; 2013: 519808.